Journal of Thermal Analysis and Calorimetry, Vol. 71 (2003) 291–310

CALORIMETRIC METHODS APPLIED TO THE INVESTIGATION OF DIVIDED SYSTEMS IN COLLOID SCIENCE

S. Lagerge[1*], *A. Kamyshny*[2], *S. Magdassi*[2] *and S. Partyka*[1]

[1]Laboratoire des Agrégats Moléculaires et Matériaux Inorganiques, CNRS UMR-5072, Université de Montpellier II, Case 015, 2 Place E. Bataillon, 34095 Montpellier Cedex 05, France
[2]Casali Institute of Applied Chemistry, The Hebrew University of Jerusalem, 91904, Israel

Abstract

A new batch titration microcalorimeter has been used for estimation of thermodynamic properties in various investigated colloidal systems. As examples, we present enthalpic and kinetic data obtained from this calorimetric device for four different processes widely encountered in colloid science:

(i) The dilution/micellization process of cationic gemini surfactants in aqueous solution.
(ii) The hydration process of non ionic surfactants in organic solution, i.e. the mechanism of micellar solubilization of water in the aggregates.
(iii) The complexation of calcium ions by polyacrylates sodium salts (PaNa).
(iv) The adsorption phenomenon of PaNa molecules on the calcium carbonate surface.

Keywords: adsorption, aggregation, biotechnology, calorimetry, colloid science, complexation, interface, micellisation

Introduction

In order to identify and quantify the phenomena which govern the different processes in colloidal systems, various methods of investigation area available; among these are the microcalorimetric methods. Thus several immersion, batch and flow microcalorimeters or calorimetric methods have been proposed for the investigation of colloids in the liquid phase [1–22]. Like most of the methods of investigation of colloidal systems in liquid phase, these microcalorimetric methods are macroscopic methods. They allow to obtain information about the following properties:

– the specific surface area of divided solids,
– the energy distribution of the surface, i.e. energetic surface heterogeneity,
– the hydrophilic – hydrophobic character (partition) of the solid surfaces,
– the chemical functions of the surface,
– the interactions between divided solids and pure liquids,

* Author for correspondence: E-mail: slagerge@univ-montp2.fr

1418–2874/2003/ $ 20.00

Akadémiai Kiadó, Budapest
Kluwer Academic Publishers, Dordrecht

– the adhesion energy,
– the interactions between adsorbate molecules and the adsorbent,
– the adsorbate-solvent and adsorbate-adsorbate interactions in the bulk phase (solution) and in the adsorbed state,
– the enthalpy of dilution and aggregation/micellisation of molecular species (surfactants, polymers…) in solution,
– the enthalpy of emulsion or microemulsion formation (solubilization of the dispersed phase in the dispersion medium),
– the adsorption kinetics,
– the thermodynamic reversibility of adsorption.

However, research on improvement of new instruments are a permanent worry of scientists in fundamental and applied research. In this paper is described a new isoperibolic microcalorimeter based on the temperature detection by Wheatstone bridge using the interchangeable very highly sensitive glass thermistors. On the world market, it is possible to select several type of microcalorimeters for which temperature variations in the calorimetric cell are usually detected by means of sensitive battery of thermocouples. Recent developments (technological and software) allowed us to imagine a new 'Calostar' batch titration microcalorimeter, which is an improved modern version of 'Montcal 3' microcalorimeter [18], so as to estimate thermodynamic properties in various investigated colloidal systems. This quite universal isothermal batch microcalorimeter consists of introducing a desired reactant from the outside of the calorimeter into a calorimetric cell which is filled by a solvent, a solution or a homogeneous particle suspension according to the desired experiment [18]. Two sensitive thermistors are immersed into the solution or suspension within the calorimetric cell and allow the temperature changes to be detected following physical or chemical reaction.

Recall that the enthalpy changes accompanying different interfacial phenomena in colloid and biological sciences can be followed by microcalorimetric batch [16, 18, 21] and flow techniques [4, 8, 12, 16, 19, 20, 22]. Several fundamental questions dealing with interfacial molecular organisation remain always to be studied. These concern the self-interactions/associations of organic and mineral ions or molecules in the bulk solution or in the interfacial region. This calorimetric method aims at following the differential molar enthalpies related with different processes such as dilution, micellization, hydration, adsorption, adsolubilisation, complexation of di- or trivalent cations by polymers... Numerous calorimetric attempts have been done as a main experimental and direct enthalpic description during the course of physical or chemical reactions while the reactions were in progress [4, 8, 12, 16, 18–22]. Thus, it is now possible to follow, step by step, physicochemical processes occurring in colloidal systems, and to measure with a very high precision the differential molar enthalpies associated with different steps. This differential view of the reactions allows to state and often draw definitive conclusions on the nature of the physical or chemical interactions occurring in the bulk phase or in the solid – liquid interfacial region. Finally, the calorimetric device described below also allows the integral heat of reaction to be measured, although this kind of information is not

as precise as differential molar enthalpies. The integral molar value gives a global picture of the phenomena which are very often composed of simultaneous or subsequent reactions. For this purpose the flow adsorption calorimeters are also currently used and give relevant results and information, especially regarding the thermodynamic reversibility of adsorption (adsorption-desorption cycles) from liquid and gas phases [4, 8, 12, 16, 19, 20, 22]. These are very sensitive and readily capable of measuring the hundredth micro-Joules [8]. The flow adsorption calorimeter determines the heat of adsorption of solute molecules from stock solutions percolating through a bed of adsorbent placed into the calorimetric cell and previously wetted by the pure solvent. The volume of calorimetric cell is usually very small (about 0.5 cc). The adsorbent can be initially evacuated *in situ* via a vacuum system (and the heat of evacuation measured) and then wetted by a pure solvent yielding the heat of wetting. The solvent is subsequently percolated at a constant flow rate and temperature, followed by an identical flow of a stock solution. When the stock solution percolates through the adsorbent bed (adsorption cycle), an endothermic or exothermic effect is detected by very sensitive thermistors which is ascribed to the adsorption process. When the thermodynamic reversibility of adsorption is studied, the pure solvent is subsequently (after the adsorption cycle) percolated through the pre-adsorbed adsorbent. If adsorption is physical in nature one usually records the opposite effect during the desorption cycle. When the interfacial process turns out to chemisorption, the reversible enthalpic effect is not observable.

Experimental device

Using the same Wheatstone bridge configuration as that used in flow microscale Adsorption Calorimeter [8] which is, in our case, monitored by a 'Eurotherm 910' instrument, a universal isoperibolical batch microcalorimeter working at temperatures ranging from 15 to 70°C has been developed. The calorimeter is schematically represented in Figs 1 and 2. The main calorimetric device of Calostar batch titration microcalorimeter embodies:

– the calorimetric cell with a total volume of 15 cc (4),
– the system of agitation (6) within the calorimetric cell (4),
– two thermistors (1) which serve to detect the temperature changes in the calorimetric cell following a reaction (dilution, aggregation, hydration, solubilization, adsorption, complexation…),
– the electrical calibration coil (3) also immersed in the calorimetric cell,
– the capillary inox inlet tube (8) which allows the stock solution of the desired reactant to be introduced from the outside into the calorimetric cell.

The special arrangement of the inlet tube (9) permits to counterbalance eventual difference in temperature between the liquid inside the calorimetric cell and the stock solution into the injection syringe (15). The homogeneity of the suspension or solution inside the calorimetric cell is ensured by the horizontal Pyrex glass stirrer (6) whose rotation speed is controlled and adapted according to the nature of the investigated system. The stirrer is indirectly connected to a stepper motor (13) fitted with magnetic transmission

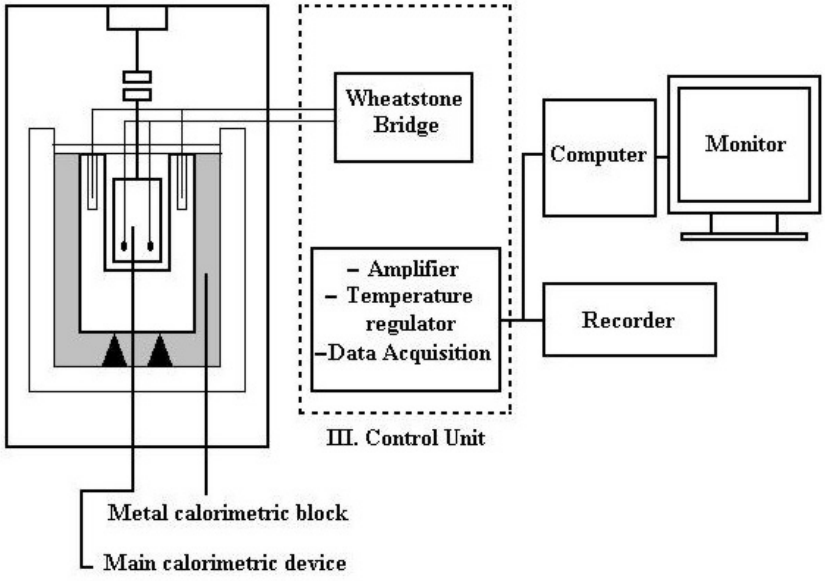

Fig. 1 Block diagram of the titration microcalorimeter and detection of the thermal effect

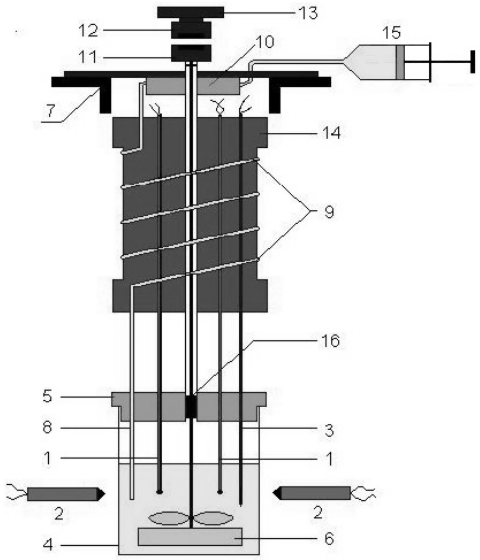

Fig. 2 Schematic representation of the calorimetric cell. 1 – measuring thermistors; 2 – reference thermistors; 3 – calibration coil; 4 – stainless steel calorimetric cell; 5 – inert cover for calorimetric cell; 6 – stirrer; 7 – aluminium block; 8 – inlet for solution injection; 9 – heat exchanger tube (plastic plug); 10 – preheater; 11 – magnet attached for stirrer; 12 – magnet attach. to electric motor; 13 – electric motor; 14 – aluminium cylinder supporting the heat exchanger tube; 15 – syringe pump; 16 – bearing

(11, 12) and placed in the external part of the calorimeter. This type of connection completely eliminates any mechanical disturbance that might be provided by the motor and is a basic requirement for the high sensitivity of the calorimeter to be kept. A precision syringe pump (15), which can be manually or automatically activated by an electronic sequencer, discontinuously injects small fractions of the stock solution into the calorimetric cell so that the corresponding differential molar enthalpies of reaction (dilution, aggregation, hydration, adsorption, complexation…) can be measured. A continuous injection allows the integral reaction enthalpies to be determined. Injection rates ranging between 0.005 and 0.20 g min^{-1} can be used without introducing any significant thermal perturbation in the system.

Table 1 Main characteristics of the Calostar titration microcalorimeter

Principle of temperature detection	Wheatstone bridge (thermistors)
Temperature working range	10–75°C
Height×diameter of calorimetric cylinder	46×31 cm
Mass of the calorimeter	15 kg
Control unit dimension	50×40×20
Time constant (τ)	30 s
Calibration resistance	≈6 Ω Power, 0.1–10 mW
Speed of agitation	100–500 rpm
Useful volume of the calorimetric cell	8–12 cm^3
Rate of injection	0.005–0.20 g min^{-1}
Instability of baseline	1 μW
Sensitivity of the temperature detectors	0.5 μV/μW
Heat production	1 μJ s^{-1}
Lowest limit of heat detection	1 mJ
Lowest limit of temperature detection	$3 \cdot 10^{-5}$°C
Stability of the baseline	several days

This main calorimetric device is placed into a metal calorimetric block whose temperature is controlled to within $5 \cdot 10^{-4}$°C. The bottom of the calorimetric cell directly contacts the metallic block. Obviously the best compromise has been found between the highest sensitivity of the calorimeter, the surface of the contact between the calorimetric cell and the metal block, and the heat capacity of the calorimetric cell content. The direct surface contact between the calorimetric cell and the metal block allows a rapid transfer of the heat from the calorimetric cell contents to the calorimetric block. Consequently, the return of the thermal signal, due to any reactions inside the calorimetric cell, to the initial baseline is very rapid (less than one hour), as observed through the thermal calibration peak produced by the Joule effect. This cali-

bration method of the calorimeter has been previously described [8]. The rapid heat loss from the cell lowers the sensitivity of the calorimeter which thereby may constitute an inconvenience. This important characteristic of the titration microcalorimeter also permits investigations on the kinetic of reactions. Conversely the introduction of suitable thickness-adjustable insulating barriers between the calorimetric cell and the metal block cell increases the sensitivity of the calorimeter together with the time of the return of the thermal signal to the initial baseline.

The time constant, τ, of the calorimeter depends on the cell-block contact quality and on the heat capacity of the calorimetric cell content.

The power dissipated in the cell at a given time, i.e. the heat evacuation from the cell at a given time is represented by the relation;

$$W=\Gamma\left(\Delta\theta+\frac{C}{\Gamma}\frac{\partial\Delta Q}{\partial t}\right) \quad (1)$$

where C and Γ are the calorific capacity and the conductance of the cell which permits the thermal equilibrium to be established, respectively, $\Delta\theta$ is the difference of temperature between the calorimetric cell and the calorimetric block.

If Γ decreases, the time constant, $\tau=C/\Gamma$, increases and for a limited period of time the temperature of the cell remains more elevated than that of the block.

This whole home-made calorimeter is fully automatically monitored. The main characteristics are gathered in Table 1. The computer controlled Calostar has a very high sensitivity, a low time constant (≈30 s), an effective volume of the calorimetric cell, a calibrated rate of injection volume of liquid reactant, a relatively fast return to the initial baseline after the reaction.

Experimental procedures

The enthalpy changes accompanying a chemical or physical reaction, for instance the dilution, aggregation, micellisation, hydration, complexation, adsorption of molecular species (electrolytes, surfactants, polymers…) can be measured by the above described isothermal microcalorimetric batch technique. This titration calorimeter allowed the species to be introduced from the outside of the calorimeter into the calorimetric cell containing a solvent, a solution or a homogeneous suspension of divided solid in the solvent [18]. It is thus possible to follow the process step by step and detect enthalpy changes associated with subsequent steps. The variation of temperature in the cell due to chemical or physical effects are detected by the thermistors arranged as in the Microscale flow calorimeter [8].

Dilution, micellization

The microcalorimeter is extremely sensitive and perfectly adapted for measuring heats of dilution. The following procedure is used for measuring an enthalpy of dilution. The calorimetric cell is filled with the solvent (about 8 g) and the injection syringe with a stock

solute solution, denoted C_0 of known molality. Once the calorimeter has reached the thermal equilibrium (after about 10 h), one aliquot of the stock solution (from 5 to 100 μL) is injected into the calorimetric cell containing the solvent. Very often, the dilution equilibrium is quasi-instantaneous, and the resulting effect is recorded. After return to the baseline (about 15 min after injection), one proceeds another injection and so on until the desired concentration in the calorimetric cell.

For the calorimetric experiments of hydration, a stock solute (surfactant) solution (about 8 g) denoted C_0 of known molality, is placed in the calorimetric cell while pure water is introduced from the outside into the calorimetric cell by small fractions using the syringe.

The apparent differential molar enthalpies of dilution ($\Delta_{\text{dil.}}\dot{h}$) and hydration ($\Delta_{\text{hydr.}}\dot{h}$), corresponding to a given dilution or hydration step were evaluated by means of the following approximations:

$$\Delta_{\text{dil.}}\dot{h}=\frac{\Delta_{\text{exp.}}H}{\Delta n_2^{\text{i}}} \quad \text{and} \quad \Delta_{\text{hydr.}}\dot{h}=\frac{\Delta_{\text{exp.}}H}{\Delta n_2^{\text{i}}} \tag{2}$$

where $\Delta_{\text{exp.}}H$ is the experimentally measured enthalpy change, n_2^{i} is the number of moles of solute or water injected into the calorimetric cell, $\Delta_{\text{dil.}}\dot{h}$ is the differential molar enthalpy of dilution for the concentration C of TX-35 in the calorimetric cell and $\Delta_{\text{hydr.}}\dot{h}$ is the differential molar enthalpy of hydration for the given hydration ratio, $w_0=\frac{n(\text{H}_2\text{O})/\text{mol}}{n(\text{TX-35})/\text{mol}}$, in the calorimetric cell. Δn_2^{i} is the number of mole of solute or water injected between the injections i and (i–1).

Adsorption process at solid-liquid interfaces

The second important contribution of the titration microcalorimeter to the study of the divided or colloidal systems concerns the enthalpy exchange when there is a transfer of molecules or ions from a solution to an interface. We will also present results connected with the adsorption of molecular species (surface active molecules, ions…) on solid surfaces. Calostar microcalorimeter remains fully suitable to study adsorption phenomena at solid–liquid interface, i.e. to measure the enthalpy changes accompanying the adsorption (transfer) of molecular species onto divided solid. In this case, the adsorbing species are introduced from the outside of the calorimeter into the calorimetric cell containing a homogeneous suspension of divided solid in the solvent. The suspension is maintained in a homogeneous state by an effective agitation. The differential molar enthalpies associated with the subsequent adsorption steps and thereby corresponding to any change in the adsorbed phase during its formation are calculated from the experimentally measured enthalpy changes, taking the effect of dilution into account. Indeed, a correction term arising from the dilution of the adsorbing species injected into the calorimetric cell should be subtracted from the total measured enthalpic effect. The enthalpy change upon adsorption will be called

henceforth the enthalpy of displacement by reason of the competitive character of the phenomenon. Therefore, dilution enthalpies of stock solutions used for adsorption have also to be determined in order to correct the values measured during the adsorption experiments for the heats of dilution. Data analysis by means of enthalpy and thermodynamic formulation of adsorption phenomena at the solid/liquid interface has been widely discussed in the literature [23].

The apparent differential molar enthalpies of displacement ($\Delta_{1,2}\dot{h}$), corresponding to a given adsorption step is evaluated according to the following equation:

$$\Delta_{1,2}\dot{h}=\frac{\Delta_{\text{exp.}}H-n_2^{\text{i}}\Delta_{\text{dil.}}h}{\Delta n_2^{\text{a}}} \tag{3}$$

where $\Delta_{\text{exp.}}H$ is the experimentally measured enthalpy change, $\Delta_{\text{dil.}}\dot{h}$ is the differential molar enthalpy of dilution for the concentration C of adsorbing species in the calorimetric cell, n_2^{i} is the number of moles of solute injected into the calorimetric cell, Δn_2^{a} is the change in the number of moles of solute adsorbed on the surface and is determined graphically with the aid of the adsorption isotherm, and $\Delta_{\text{dil.}}h$ is the molar integral enthalpy of dilution for the equilibrium concentration of adsorbing species in the calorimetric cell.

It is important to recall that the total variation of the experimental enthalpy of displacement includes not only the adsorption energy of the adsorbate molecule but also some other energetic contributions. These energetic contributions arise from the desorption (displacement) of the water molecules from the surface following the adsorption of molecular species, from the dehydration of the adsorbed organic species, from the desorption of exchanged mineral ions and from their rehydration in the bulk phase. Structuration/destructuration effects of the adsorbed species at the interface and in the bulk phase and other energetic contributions arising from, for instance, the aggregation when the concentration in the aqueous phase is upper than the critical concentration of aggregation have also been considered in the displacement enthalpy.

Hydration, micellar solubilization, and complexation processes

The experimental procedures are very similar to those above described for the dilution and adsorption experiments. The only small differences will be mentioned before presenting the experimental results in the following section.

Some results and concluding remarks

Since our paper aims at presenting an outline of the potential of the 'Calostar' titration microcalorimeter, we are confining it to the phenomenological observations demonstrated by the curves, characterising variations of the enthalpies for arbitrarily selected systems. Only concluding remarks will be mentioned here. For more detailed explanations of the investigated phenomena, we give references of the related papers that have been already published elsewhere.

Dilution process of cationic Gemini surfactants in aqueous solution: thermodynamics of the aggregation/micellization process [26, 27]

The enthalpies of dilution of micellar solutions of several dimeric cationic surfactants of the alkanediyl-α,ω-bis(dodecyldimethylammonium bromide) type, referred to as 12–*s*–12, and of a classical cationic surfactant, dodecyltrimethylammonium bromide (DTAB) have been measured calorimetrically, in a range of concentrations extending from well below to well above the critical micelle concentration (*cmc*). The chemical structures of the surfactants are reported in Fig. 3. In Table 2 are listed their *cmc* and the micelle ionisation degree values (α) in pure water. The dimeric cationic surfactants differ by the carbon number *s* of the alkanediyl spacer. The calorimetric results permit the determination of the enthalpy of micellization, $\Delta_{mic}h$, of the investigated surfactants at 25 and 35°C.

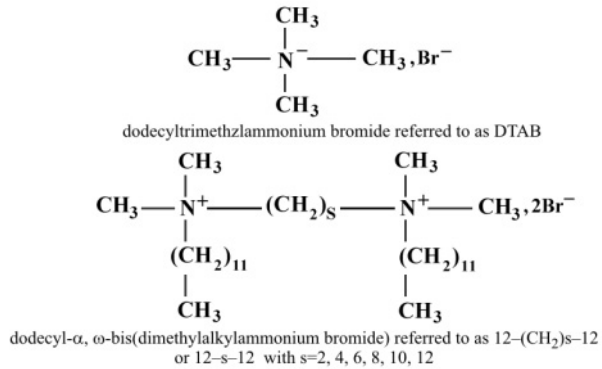

Fig. 3 Chemical structures of the conventional and dimeric cationic surfactants

Table 2 Values of the critical micellar concentration (*cmc*) of the investigated surfactants and dissociation degree (α) of the counter-ion (Br^-) to the corresponding micelles at 298 K

	DTAB	12–2–12	12–4–12	12–6–12	12–8–12	12–10–12	12–12–12
cmc/mM[a]	14	0.84	1.17	1.03	0.83	0.63	0.37
α[b]	0.20	0.16	0.16	0.20	0.25	0.26	0.31

[a]From [24a]
[b]Calculated from conductivity data using the method of Evans in [25]

All the calorimetric experiments were performed using a stock solution of surfactant at a concentration C_0 about 10 to 15 times larger than the *cmc*. Figure 4 illustrates the variation of the differential molar enthalpy of dilution, $\Delta_{dil}h$ with the analytical surfactant concentration *C* in the calorimetric cell, obtained following successive injections of surfactant stock solution, at 35°C. The measured enthalpies of dilution are positive, indicating an endothermic process in the whole range of concentration. Similar results (shape of the curve and positive enthalpic values) were obtained

at 25°C and for all the other surfactants. Three ranges can be distinguished in the plot in Fig. 4.

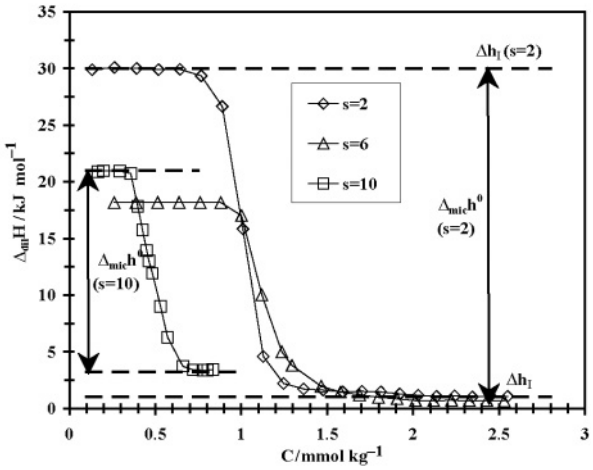

Fig. 4 Variation of the differential molar enthalpy of dilution of 12–2–12, 12–6–12 and 12–10–12 at 308 K

(i) In the first plateau region, the surfactant concentrations are lower than the *cmc*. The injections result in a quite constant and strongly endothermic effect, Δh_I. This enthalpic effect results, on the one hand, from the dissociation of all the micelles (initially in the stock solution) introduced in the cell, i.e. first in pure deionised water (first injection) and then in solution of surfactant monomers of concentration lower than the *cmc* in the calorimetric cell, and, on the other hand from the dilution of these resulting individual surfactant molecules water. The dissociation of micelles is endothermic and constant (Δh_I). Consequently, the opposite process (micellization process) is exothermic ($\Delta_{dil.}h_{(final)}-\Delta_{dil.}h_{(initial)}=\Delta h_{III}-\Delta h_I$).

(ii) The second enthalpic region ($\Delta_{dil}h$) corresponds to the sharp declining part of the dilution curve in the *cmc* range. It is attributed to the 'formation' and dilution of micelles in the calorimetric cell. Indeed, the subsequent injections of stock solution lead to an increase of the concentration in the calorimetric cell, and from a particular value, less and less surfactant monomers are removed from the initial injected micelle upon the dilution. In such a case, the corresponding enthalpic effect of dilution sharply decreases and becomes less and less endothermic because the injected micelles are less and less dissociated in the calorimetric cell following the dilution. Moreover, by injecting a high concentration stock solution into the calorimetric cell, numerous processes and equilibria, due to the evolution of the average size of the aggregates (aggregates distribution) involving both their size and their number may occur, including the following:

– dilution of aggregates and monomers originally present in the syringe (stock solution)
– solvation/desolvation of the produced species (monomers, dimers and aggregates).

(iii) Above the *cmc*, once the maximal aggregation number is reached, the injections result in a quite constant and weakly endothermic effect, Δh_{III}, which is ascribed to the dilution of the stock micellar solution (micelles of given average size in the syringe) into a more diluted micellar solution in the cell. The subsequent enthalpy will remain constant and close to zero.

The same behavior is observed for all surfactants at 25 and 35°C. The enthalpy of micellization at the *cmc* is taken as;

$$\Delta_{mic}h=\Delta h_{III}-\Delta h_{I}\approx\Delta_{mic}h^{0} \quad (4)$$

In Eq. (4) the enthalpy of micellization at the *cmc*, $\Delta_{mic}h$, has been assumed to be equal to the standard enthalpy of micellization, $\Delta_{mic}h^{0}$, because the *cmc* value are small (close to or below 1 mM). All the $\Delta_{mic}h^{0}$ values obtained in this way are negative, indicating that micelle formation is an exothermic process for the investigated surfactants. The values of $-\Delta_{mic}h^{0}$ are plotted in Fig. 5 as a function of *s* at *T*=25°C and *T*=35°C. In this figure we have also reported the effect of the spacer *s* on the *cmc* at 25°C. The effect of the spacer carbon number is seen to be very important. The measured $\Delta_{mic}h^{0}$ are strongly dependent on the spacer carbon number. Thus $-\Delta_{mic}h^{0}$ decreases significantly as *s* is increased from 2 to 4 and goes through a rather flat minimum at *s* between 4 and 6. The increase of $-\Delta_{mic}h^{0}$ for $s\geq6$ is small but note worthy. Also noteworthy is the much larger value of $-\Delta_{mic}h^{0}$ for 12–2–12 with respect to DTAB, even when taking into account the fact that the surfactant dimer contains two dodecyl chains. Finally, the measured enthalpies all become more negative as the temperature is increased, a behavior previously reported for many conventional surfactants. The strongly negative value of $\Delta_{mic}h^{0}$ for 12–2–12 appears to be due to the sterically hindered rotation of the surfactant alkyl chains around the spacer C–C bond. This effect is much weaker or not present for the 12–*s*–12 surfactants with *s*>5.

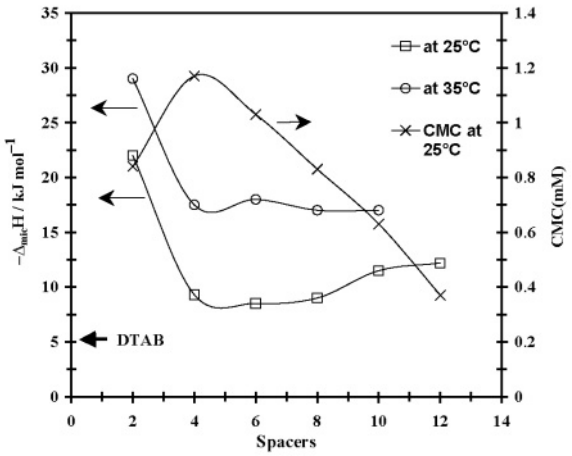

Fig. 5 12–*s*–12 surfactants: Effect of the spacer carbon number *s* on the *cmc* at 25°C and on the enthalpy of micellization at 298 and 308 K. The arrow (at the bottom on the left) indicates the enthalpy of micellization of DTAB at 298 K

Table 3 Enthalpies, specific heats, free energies and entropies of micellization for the investigated surfactants at 298 K

	DTAB	12–2–12	12–4–12	12–6–12	12–8–12	12–10–12	12–12–12
$\Delta_{mic}h^0$/kJ mol^{-1}	–1.7	–22	–9.3	–8.5	–9	–11.6	–12.2
$\Delta_{mic}C_P^0$/kJ mol^{-1} deg^{-1}	–0.23	–0.65	–0.84	–0.9	–0.83	–0.71	–0.76
$\Delta_{mic}g^0$/kJ mol^{-1}	–19.1	–47.3	–45.1	–44.6	–44.2	–45.5	–46.8
$T\Delta_{mic}s^0$/kJ mol^{-1}	17.4	25.3	35.8	36.1	35.2	33.9	34.6

The isobaric specific heats of micellization, $\Delta_{mic}C_p^0$ can be calculated from the values of $\Delta_{mic}h^0$ at 25 and 35°C according the following relationship;

$$\Delta_{mic}C_p^0 = \left(\frac{\partial \Delta_{mic}h^0}{\partial T}\right)_p \quad (5)$$

Moreover the values of the free enthalpy of micellization, $-\Delta_{mic}g^0$ [24b], and of the entropy of micellization, $-\Delta_{mic}s^0$, can be obtained from the following equations:

$$\Delta_{mic}g^0 = 2RT(1.5-\alpha)\ln cmc \quad (6)$$

$$T\Delta_{mic}s^0 = \Delta_{mic}h^0 - \Delta_{mic}g^0 \quad (7)$$

where α is the micelle ionisation degree. These α values, reported in Table 2, have been calculated for all the investigated surfactants according to the Evans' method [24a, 25] with a micelle aggregation number of 50 [28]. All these calculated thermodynamic properties (expressed per mole of surfactant) are listed in Table 3.

The $\Delta_{mic}C_p^0$ values are all negative. It is seen that $-\Delta_{mic}C_p^0$ varies relatively little with the spacer carbon number, contrary to $\Delta_{mic}h^0$, and that $-\Delta_{mic}C_p^0$ is a maximum at *s* around 6. The values of $-\Delta_{mic}C_p^0$ for 12–4–12, 12–6–12 and 12–8–12 are all larger than twice the value for DTAB. The difference may associate to the presence of the spacer in the surfactant dimers. The values of $\Delta_{mic}g^0$ and of $\Delta_{mic}s^0$ give additional information on the thermodynamics of micellization of 12–*s*–12 surfactants. For all the surfactants investigated, the results show that $T\Delta_{mic}s^0 > -\Delta_{mic}h^0$ indicating that the micellization of dimeric surfactant is entropy-driven, as for conventional surfactants.

This work illustrates the usefulness of the microcalorimetricity investigations of micellar solutions of surfactants for a better understanding of the behavior of these systems.

Hydration process of non-ionic surfactants in organic solution: thermodynamics of the micellar solubilization of water [29]

The behaviour of a non-ionic surfactant TX-35 in solution in *n*-heptane in the presence and in the absence of added water has been examined using the microcalorimetric experimental methods. The polydisperse non-ionic surfactant, TX-35 is a poly(oxyethylene) octyl-phenol with an average ethylene oxide chain composed of 3 segments ($C_8\Phi EO_3$). The TX-35 molecules are soluble in *n*-heptane to a great extent. For non-ionic surfactants in organic solvents, we have to consider 'an operational CMC' from which the surfactant molecules begins to aggregate in oil phase by analogy to the CMC in aqueous solution. Careful investigations on reverse micelles have shown that only the concept of 'an operational CMC' is applicable in non-polar solvents. First, the analysis of the differential molar enthalpies of dilution of TX-35 in dried *n*-heptane, determined according to the same method as above for Gemini surfactants, has shown the occurrence of a gradual exothermic aggregation process on a very wide range of concentration which takes place at the particular concentration so-called 'operational CMC'. We were also interested in the solubilization process of water in the reverse micelle of the poly(oxyethylene) glycol

alkylphenyl ether surfactant (micellar solubilization). Microcalorimetric experiments of hydration/solubilization have been carried out using a TX-35 stock solution of 0.5 mol kg^{-1}. This solution is placed in the calorimetric cell while the pure water is introduced from the outside to the calorimetric cell by fraction of 25 μL using the syringe. At this TX-35 concentration, the solution contains optimal reverse micelles which are able to solubilize water.

Figure 6a shows the evolution of the differential molar enthalpy of hydration as a function of w_0. The corresponding enthalpic curve is gradually decreasing. The differential molar enthalpy of hydration was found to be exothermic; $(\Delta_{hydr.}\dot{h})_{w=0} \approx -8$ kJ per mole of TX-35. It is particularly interesting to note that for $w_0 \approx 3.2$ moles H_2O per mole of TX-35, the thermal effect becomes zero. This particular value of hydration ratio corresponds to the point of phase separation and corresponds to the maximal hydration ratio or water solubilization capacity as confirmed by direct measurement of the quantities of water contained in the TX-35 solutions at different concentrations. Moreover, in Fig. 6b, one notes that the time (t) necessary to get back to the thermal equilibrium, after each injection, increases spectacularly as fast as w_0 is increasing and stabilize when the hydration is finished. This suggests that the kinetic of water solubilization in reverse micelles is significantly increased with increasing w_0. The rate of solubilization of additional water decreases with increasing amount of water already present in the aggregates (approach of saturation and phase separation). The microcalorimetric experiment of hydration/solubilization can therefore be used not only for $\Delta_{hydr.}\dot{h}$ determination but also as a relevant method for the quantification of water solubilization in reverse micelles. For $w_0 < 3.2$, two phenomena superimposed and have to be considered. When water is introduced in the stock solution of 0.5 mol kg^{-1}, first it occurs an endothermic effect due to the so-called hydrophobic hydration [30]. In the calorimetric experiments, this hydrophobic hydration effect is present during each injection of pure water in *n*-heptane solution. Then, in a second step, most part of the added water molecules are transferred from *n*-heptane saturated by water to the reverse micelles of TX-35. This second phenomenon consists in the solubilization of fresh water in a 'hydrophilic core' made up of the poly(oxyethylene) groups of the surfactant. It is not easy to establish how much energy is liberated during this second step but it is evident that the resulting thermal effect is exothermic and probably quite constant. Moreover, solubilization of water in the reverse micelle probably leads to their swelling and therefore to an increase of their size, until full saturation. This phenomenon of swelling of the aggregates favours the interactions between *n*-heptane and polar parts (water or (EO) groups). Consequently, some surfactants still present as individual monomers in the solution may 'adsorb' or aggregate on the existing reverse micelle in order to decrease the water-*n*-heptane interactions and therefore to stabilize the aggregate. In such a case the adding of water leads to an increase of the aggregation number. This later process is exothermic and decreasing, according the dilution experiments which show that the gradual desaggregation or dissociation is less and less endothermic. The measured total thermal effect is therefore the sum of the solubilization of water (which is probably exothermic and quite constant) and the aggregation process which is less and less exothermic.

These two superimposed phenomena can support the trend of the microcalorimetric hydration curve reported in Fig. 6a. The progressive evolution of the aggregates is highlighted by kinetic data (Fig. 6b). The hydration is very fast up to $w_0 \approx 1.5$, then it becomes much more slower. These kinetic data can also be interpreted as a change of the aggregates shape. Indeed, the first water molecules are transferred from *n*-heptane to the dimers or trimers and are directly bonded to the EO groups (hydration process). The size of the aggregates are increasing and it is justified to think that the subsequent water molecules are solubilized into the already pre-existing aggregates. This qualitative and gradual changing in shape and consequently in diameter occurs for w_0 ranging between 1.5 and 2 (Fig. 6b). This noticing has been confirmed by viscosity and light scattering investigations.

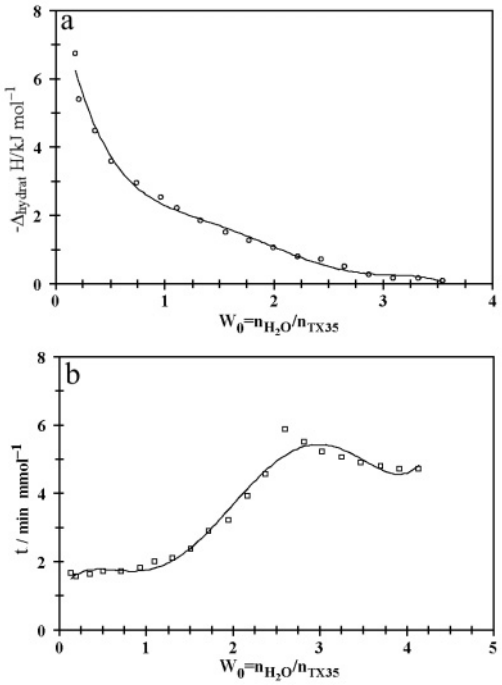

Fig. 6 a – Differential molar enthalpies of hydration of TX-35 ($\Delta_{hydrat.}\dot{h}$ in kJ mol^{-1} of surfactant) and b – time of half-return to the baseline of the calorimetric signal (t in min per number of millimoles injected) *vs.* the molar hydration ratio $\left(w_0=\frac{n(H_2O)}{n(\text{TX-35})}\right)$ at T=298 K (C_0=0.466 mol kg^{-1})

The conclusions drawn from these titration microcalorimetric results are all very well supported by other experiments; These very well corroborate viscosimetric, light scattering, and titration of water data for the determination of the operational CMC and for the quantification of the micellar solubilization of water [29].

Enthalpy of interaction or binding between Ca^{2+} divalent cations and polyacrylate sodium salt: complexation process [31, 32]

The enthalpy changes following the addition of Ca^{2+} ions to a polyacrylate sodium salt (PaNa) solution were also determined. The experimental procedure is similar to that used in the dilution experiments. In the complexation experiments the injection syringe is filled with a 10^{-1} M $CaCl_2$ stock solution and the calorimetric cell contains a 1 g kg^{-1} PaNa solution in deionized water. PaNa of different molecular masses (1200, 2100, 5100, 15000 g mol^{-1}) were investigated. Following injection of small fractions of $CaCl_2$ solution in the calorimetric cell, we can assess the enthalpic effect related to the complexation of Ca^{2+} ions by the carboxylate groups of PaNa. The enthalpy change accompanying the reaction taking place between PaNa and the divalent ions is denoted $\Delta_{compl}H$, and this was corrected for the enthalpy of dilution associated with the injection of a 10^{-1} M $CaCl_2$ solution into pure deionised water. The contribution of the enthalpy of dilution, $\Delta_{dil}H$, to the total enthalpy change was almost zero. The enthalpy of complexation, $\Delta_{compl}h$ in kJ mol^{-1}, was calculated according to the equation:

$$\Delta_{compl}h = \frac{(\Delta_{exp}H - \Delta_{dil}H)}{n_{Ca}^{inj}} \tag{8}$$

where $\Delta_{dil}H$ denotes the experimental enthalpy of dilution of the $CaCl_2$ solution in deionised water and $\Delta_{exp}H$ denotes the experimental enthalpic value detected following injection of $CaCl_2$ in the PaNa solution. n_{Ca}^{inj} represents the quantity of Ca^{2+} ions injected in the calorimetric cell (expressed in moles).

Figure 7 shows the observed enthalpy effect following injection of Ca^{2+} ions ($CaCl_2$) in the calorimetric cell. In this figure we have reported the enthalpic values expressed in kiloJoules per mole of calcium injected *vs.* the total concentration of calcium ions (free Ca^{2+}+Ca^{2+} bound to PaNa) in the calorimetric cell. The enthalpic curve indicates the occurrence of endothermic interactions between PaNa and Ca^{2+} ions; in other words, the complexation of calcium ions by PaNa is an endothermic process. The Δh values expressed in kJ per mole of calcium bound to the PaNa can be calculated using the complexation isotherm i.e. the graph $[Ca^{2+}]_{bound}=f(\text{free } [Ca^{2+}])$. This graph represents the distribution of Ca^{2+} ions between the PaNa molecules (Ca^{2+} bound) and the bulk phase (Ca^{2+} free); This isotherm has been determined but is not presented in the paper. The corresponding calorimetric plot (Δh expressed in kJ per mole of bound calcium *vs.* the complexation ratio [Ca]/[PaNa]) is a horizontal straight line, indicating that the enthalpy of complexation does not vary with the complexation ratio, i.e. that the enthalpy is constant (about 8 kJ mol^{-1}) in the whole range of complexation. The endothermic feature of the Ca^{2+}/PaNa complexation implies an entropy gain in the system, which is produced by the partial desolvation of the complexing species (Ca^{2+}) as well as the carboxylate group [33]. The loss of water accompanying the complexation of multivalent cations with polyelectrolyte has already been established [34]. Finally, it is relevant to indicate that the sudden precipitation of the polymer at the end of the complexation reaction does not lead to any heat effects.. The enthalpy curves show a similar trend for all the PaNa investigated. Each

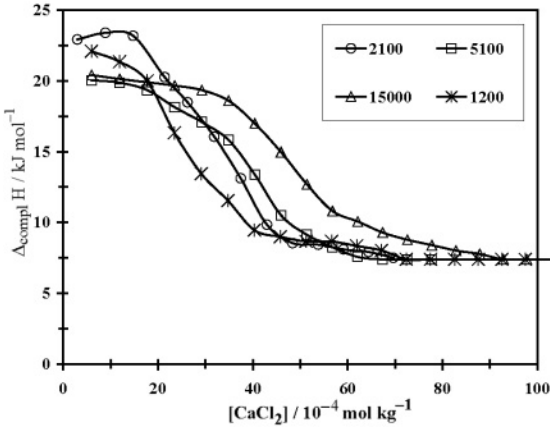

Fig. 7 Differential molar enthalpies of binding of calcium ions to the polyacrylate sodium salts at 298 K; Evolution of the complexation enthalpy

enthalpic curve presented in Fig. 7 starts at roughly the same value (about +23 kJ mol^{-1}). The different shapes are directly related to the initial $CaCl_2$ concentration in the calorimetric cell. With a 0.1 mM $CaCl_2$ solution, only very small quantities of injected $CaCl_2$ solution are necessary to bind (saturate) all the polymer available in the calorimetric cell. After three injections, the enthalpy of complexation drops gradually, indicating that less and less calcium ions are bound to the polymer. After a few injections (for $[CaCl_2]>5\cdot10^{-3}$ mol kg^{-1}, no more calcium is bound to the polymer, resulting in a constant positive enthalpy change, $\Delta_{compl}h$ (about –7 kJ mol^{-1}).

Adsorption process at solid - liquid interface: interaction between PaNa molecules and calcium carbonate [31]

To investigate the adsorption of PaNa on the calcite surface, we used a 1% mass/mass PaNa stock solution in the injection syringe. A homogeneous $CaCO_3$ suspension (3 g of calcite was dispersed into 8 g of deionized water) was placed in the calorimetric cell. However the equilibrium supernatant in the calorimetric cell contained calcium ions provided by the sparingly soluble calcium carbonate. Consequently, most of the thermal effect obtained following the injection of polymer into the calorimetric vessel was due to the complexation process between the carboxylic groups of the polymer and the calcium ions. For that reason, we previously attempted to determine the enthalpy of complexation between carboxylic groups in PaNa and Ca^{2+} ions obtained by injecting $CaCl_2$ solution into a polymer solution. Injection of PaNa molecules in a $CaCl_2$ solution gave similar results. The same calorimetric experiments of adsorption were performed in the presence of Na_2CO_3 as extra salt in the adsorption medium. Na_2CO_3 was added in the adsorption medium so as to prevent solubilization process of the calcite and thereby to study the effect of calcium ions on PaNa adsorption onto calcite. Indeed, in the presence of Na_2CO_3 (2 g L^{-1}), the solubility equilibrium of $CaCO_3$ should be shifted towards the left hand (precipitation of the solid) according the following reaction:

$$CaCO_3 \leftrightarrow Ca^{2+} + CO_3^{2-} \quad (9)$$

In Fig. 8, we compare the enthalpic evolution obtained for the adsorption PaNa (5100 g mol^{-1}) on dispersed calcium carbonate in the presence and in the absence of Na_2CO_3 in the equilibrated supernatant.. In these curves, the enthalpy of interaction, $\Delta_{exp}H$, is not corrected for the enthalpic term arising from interactions occurring in the bulk phase. This correction term corresponds to the enthalpy of dilution of PaNa in the equilibrated supernatant, including the complexation between carboxylic groups of the polymer and the free calcium ions. This correction term is not easy to assess because the calcite solubilization and thereby the bulk composition depends on the PaNa amount adsorbed.

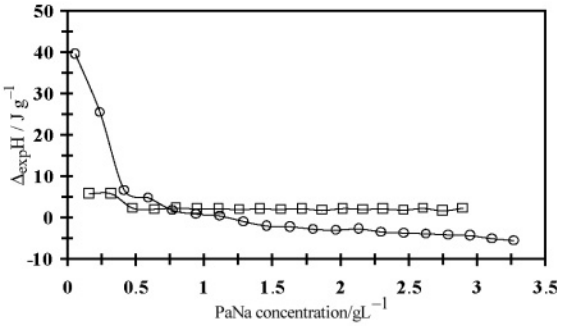

Fig. 8 Variation of the differential molar enthalpies of adsorption of polyacrylate sodium salt (M_m=5100 g mol^{-1}) onto calcium carbonate 298 K. Open circles – adsorption of PaNa from deionized water; open squares – adsorption in the presence of Na_2CO_3 as extra salt

The enthalpy curve for the adsorption of PaNa on dispersed solid in deionized water starts with highly endothermic values (which would normally be taken as an indication of an entropically driven adsorption process), and the curve then clearly shows a decrease in the enthalpy change. The enthalpic effect shows an extremely steep initial decrease (from 40 to 0 J g^{-1}) while the coverage increases. From a concentration range of 0.5 g L^{-1}, the enthalpy of interaction then gradually decreases and finally becomes fairly constant and exothermic (about – 5 J g^{-1}).

It can be concluded from the calorimetric data presented in Fig. 8 that, in contrast to the adsorption experiment in deionized water (open circles), the adsorption curve in the presence of Na_2CO_3 (open squares) does not exhibit any endothermic region. The enthalpy of interaction observed between the dispersed calcium carbonate and PaNa in the presence of Na_2CO_3 is fairly constant and the reaction is slightly endothermic (about –1 J g^{-1}) over the whole concentration range. The only significant difference between whether or not Na_2CO_3 is added in the adsorption medium, is found at low concentrations or low coverage ratios, i.e. for quantities of added polymer lower than 0.5 g L^{-1}. Quite the same exothermic value as that obtained at high polymer concentrations in the absence of Na_2CO_3 is also observed in the presence of Na_2CO_3 the whole adsorption range and in the range where no adsorption was detected. This clearly indicates that the initial endother-

mic part is ascribed to the complexation of Ca^{2+} ions in the bulk phase, which disappear in the presence of Na_2CO_3 (calcite solubility is very weak) while the residual exothermicity reflect the direct adsorption of PaNa on the calcite surface. Indeed, in the absence of calcium ions in the solution, the only thermal effect is due to the direct adsorption of PaNa on the calcite surface. Thus we can conclude that the net adsorption of PaNa on the calcite surface is an exothermic process and not endothermic as we could think if the experiment in deionized water alone had been made. More important, the calorimetric results allow us to definitively state that the depletion observed on the adsorption isotherm in the range of low PaNa concentrations does not reflect an adsorption process but is essentially produced by the precipitation of the calcium-polyacrylate complexes. The amount calcium-polyacrylate precipitate was initially wrongly counted as an amount of adsorption because it is retained on the filter with the calcite particles during the filtration process. Indeed, after the equilibrium of adsorption, the calcite suspension is filtered so as to analyse the amount of PaNa remaining in the equilibrated supernatant and to calculate the amount adsorbed.

The calorimetric measurements provided valuable information concerning enthalpy changes originating from both specific surface interactions and interaction in bulk solution. It was shown that the adsorption of PaNa onto calcium carbonate is basically exothermic. Endothermic enthalpy changes were also found to occur between calcium ions present in the supernatant obtained from $CaCl_2$ solutions and the carboxylic acid groups, suggesting a complexation in the bulk solution.

Conclusions

In this paper we described four calorimetric experiments (dilution/aggregation, hydration, adsorption and complexation) which demonstrate that the isothermal titration calorimeter is particularly valuable to investigate physical or chemical reactions in divided, colloidal and biological systems. The limited scope of this report does not allow us to describe all the numerous possible applications. Moreover, since our paper aims at presenting an outline of the potential of the titration Calostar titration calorimeter, we are confining it to the phenomenological observations demonstrated by the curves, characterising variations of the enthalpies for these four arbitrarily selected systems. This calorimeter also proved to be particularly suitable to determine relevant and complementary quantitative information on many other processes related with colloid science. For instance, polymer-surfactant systems (interactions), oil solubilization in supramolecular aggregates have also been successfully investigated. In both cases, the measured enthalpies and the calculated thermodynamic properties (entropy, free energy…) allowed to get an insight into the nature of the interactions and to give a complementary description on the mechanisms of reaction.

References

1 W. D. Harkins and G. Jura, J. Am. Chem. Soc., 66 (1944) 1362.
2 E. Calvet and H. Prat, Récents Progrès en Microcalorimétrie, Pergamon, New York 1963.

3 T. Morimoto and H. Naono, Bull. Chem. Soc. Jpn., 37 (1964) 392.
4 A. J. Groszek, ASLE Trans., 9 (1966) 67.
5 J. M. Corkill, J. F. Goodman and J. R. Taste, Trans. Faraday Soc., 62 (1966) 979.
6 A. C. Zettlemoyer, J. Colloid Interface Sci., 28 (1968) 343.
7 D. H. Everett and G. Findenegg, J. Chem. Thermodyn., 1 (1969) 573.
8 A. J. Groszek, Proc. R. Soc. London Ser. A, 314 (1970) 473.
9 C. Letoquart, F. Rouquerol and J. Rouquerol, J. Chim. Phys., 70 (1973) 559.
10 D. H. Everett, Isr. J. Chem., 14 (1975) 267.
11 A. K. Miles and J. A. Hockey, J. Chem. Soc. Faraday Trans., 1, 71 (1975) 2392.
12 S. Partyka, F. Rouquerol and J. Rouquerol, J. Colloid Interface Sci., 68 (1979) 1.
13 J. E. Desnoyers, R. Delisi and G. Perron, Pure Appl. Chem., 52 (1980) 433.
14 R. Denoyel, F. Rouquerol and J. Rouquerol, in C. Rochester (Ed.), Adsorption from Solution, Academic Press, London 1982, p. 225.
15 G. W. Woodbury and L. Noll, Colloids Surfaces, 8 (1983) 1.
16 J. Rouquerol, Pure Appl. Chem., 57 (1985) 67.
17 S. Partyka, M. Lindheimer, J. Y. Bottero, B. Brun and P. Somasundaran, Cal. Ther., 16 (1985) 76.
18 S. Partyka, M. Lindheimer, S. Zaini, E. Keh and B. Brun, Langmuir, 2 (1986) 101.
19 G. Findenegg and M. Liphard, Carbon, 25 (1987) 119.
20 G. W. Woodbury and L. Noll, Colloids Surfaces, 28 (1987) 233.
21 S. Partyka, E. Keh, M. Lindheimer and A. J. Groszek, Colloids Surfaces, 37 (1989) 309.
22 S. Lagerge, J. Zajac, S. Partyka and A. J. Groszek, Langmuir, 15 (1999) 4803.
23 Z. Kiraly, I. Dekany and L. G. Nagy, Colloid Surf., 71 (1993) 287.
24 (a) R. Zana, M. Benrraou and R. Rueff, Langmuir, 7 (1991) 1072.
(b) R. Zana, Langmuir, 12 (199) 1208.
25 H. C. Evans, J. Chem. Soc., 559 (1956)
26 L. Grosmaire, M. Chorro, C. Chorro, S. Partyka and R. Zana, J. Colloid Interface Sci., 246 (2002) 175.
27 L. Grosmaire, M. Chorro, C. Chorro, S. Partyka and S. Lagerge, Thermochim. Acta, 379 (2001) 255.
28. D. Danino, Y. Talmon and R. Zana, Langmuir, 11 (1995) 1448.
29 S. Lagerge, E. Grimberg-Michaud, K. Guerfi and S. Partyka, J. Colloid Interface Sci., 209 (1999) 271.
30 C. Tanford, 'The Hydrophobic Effect', Wiley, New York 1973., Chap. 8, p. 43.
31 K. Backfolk, S. Lagerge, J. B. Rosenholm and D. Eklund, J. Colloid Interface Sci., 248 (2001) 5.
32 I. Pochard, A. Foissy and P. Couchot, Colloid Polymer Sci., 277 (1999) 818.
33 M. R. Bohmer, Y. El Attar Sofi and A. Foissy, J. Colloid Interface Sci., 164 (1994) 126.
34 M. Satoh, M. Hayashi, J. Komiyama and T. Lijima, Polymer, 31 (1990) 501.